Journal of Earth Science, 2018; Vol. 29, No. 6, p. 1431–1442 ISSN 1674-487X
Printed in China
https://doi.org/10.1007/s12583-018-0883-4 Online ISSN
1867-111X

Paleoproterozoic Underwater Volcanism and Microfossil-Like Structures in the Metasedimentary Siliceous Rocks, Hogland Island, Russia

Anatoly M. Belyaev *
Institute of Earth Sciences, St. Petersburg State University, St. Petersburg 199034, Russia
Anatoly M. Belyaev: https://orcid.org/0000-0001-7035-7521

ABSTRACT: Geological surveys showed that rhyolite and basalt strata with pillow structures typical for underwater volcanism form sheets over the Svecofennian basement. Original geochemical and isotope-geochemical data confirmed that the rhyolites were formed contemporaneously with the rapakivi granites of the Wiborg Massif (1 640 Ma), and the basalts are similar to gabbro-anorthosites. Abnormally high content of K2O and relatively low content of Na2O in rhyolites and basalts are interpreted as a result of hydrothermal interaction of eruptive magmas with K-enriched hot seawater. The strata of siliceous metasedimentary rocks (microquartzites) within basaltic and rhyolitic lavas were formed in processes of chemogenic sedimentation and subsequent contact metamorphism during underwater volcanism. Microquartzites showed carbon vastly depleted of heavy isotope 13C. This is typical for rocks formed with participation of living substance. The Raman spectra of the remaining carbon-containing substance have graphite bands. In the microquartzites among basalts and rhyolites we found a community of structures with external and internal morphology similar to modern or fossilized marine microorganisms: spiral cyanobacterias, amoebas, diatoms, foraminifers, virus capsids, flagellates and multicellular organisms. It is assumed that these silificated and ferruginizated microfossils represent the Paleoproterozoic community of marine microorganisms.

KEY WORDS: submarine volcanism, siliceous rocks, silification, Paleoproterozoic microfossils, carbon isotopes.

0 INTRODUCTION

The new finds of ancient microfossils are important for understanding the origin and evolution of life on Earth. In this case, it is necessary to study the general geological environment to reconstruct the sedimentation and fossilization conditions (Rozanov, 2002). Remains of non-skeletal aquatic organisms with their morphology well preserved due to silification are known in modern thermal springs with high concentration of chemogenic siliceous sediments (Rozanov, 2002). The experiments proved that in such an environment the silification of aquatic organisms (Benning et al., 2002; Westall et al., 1995) and even viruses (Orange et al., 2011) occurs quite fast, driven by water temperature and silicon content (Renaut et al., 1998). Similar conditions occurred during underwater volcanic activity, when the sea water, heated by lava, was saturated with silica, dissolving the silicate material from the lava flows. It was favorable for fast silification and created ferruginous conditions during burial of planktonic marine microorganisms in the siliceous sediments. The overlap of these sediments with hot lava flows led to their transformation in metasedimentary siliceous rocks as the result of contact metamorphism.Therefore, the ancient chemogenic siliceous rocks, formed in the processes of underwater volcanism, are very promising for the discovery of new well preserved silificated and ferruginous microfossils.
In this work we present data on the petrology of Paleoproterozoic submarine volcanism and reconstruct the environment, which defined the structure of microfossil in the metasedimentary siliceous rocks.

1 MATERIALS AND METHODS

Igneous and metasedimentary rocks were studied using various physical and chemical methods for identification of signs of life. These investigations were performed in certified laboratories using licensed equipment and software.

Polished samples and thin sections of siliceous rocks were studied using optical and scanning transmission electron microscopy methods. Powdered samples of Microquartzites were subjected to X-ray diffraction exploration, isotopic geochemical and Raman micro-spectroscopic studies.

X-ray spectral fluorescence analysis of chemical composition of magmatic and metasedimentary rocks was carried out in the Central Laboratory of the Russian Geological Research Institute, St. Petersburg. Accreditation certificate No. POCC RU.0001.510415.

Chemical composition of minerals was determined in the Institute of Precambrian Geology and Geochronology of the Russian Academy of Sciences using scanning electron microscope JSM-6510LA with energy-dispersion spectrometer JED-2200 (JEOL, Japan). The photos of microfossils of similar objects were taken in compositional contrast mode-reflected (BEC) and secondary electrons (SEI).

X-ray diffraction study of the mineral composition of the microquartzites from powdered samples was carried out in the Center of the X-ray Diffraction Analysis of St. Petersburg State University using Bruker's D2 Phaser Diffractometer (Germany).

Petrographical microscopic exploration and photos of polished samples and thin polished sections were carried out in the Institute of Earth Sciences of St. Petersburg State University using polarizing microscopes MIN-8, MIN-9, MBS-2 (LOMO, St. Petersburg, Russia), and polarizing microscope Leica LP with digital camera DFC420&SW (Leica Microsystems, Germany).

Analyses of stable carbon isotopes in microquartzites from basalts and rhyolites were carried out in the Isotopic Research Center of the Russian Geological Research Institute using elementary analyzer Flash EA 1112 (ThermoQuest, Milano, Italy), and multi-collector mass-spectrometer DELTAPlus-XL (Thermo-Finnigan, Germany) with gas communicator ConFlo III (Thermo-Finnigan, Germany). Powdered samples of microquartzites were decarbonized using HCl/HF mixture at 100-180 ·C, washed in ultra-pure water and neutralized by H3BO3. The balance of stable isotope was calculated as: δ13C (‰)=1 000× {(13C/12C) sample/(13C/12C)PDB · 1}, where PDB is the international Pee Dee Belemnite standard. The reproducibility and accuracy of this method, in comparison with various working standards, was within ±0.2‰. For analysis of carbon isotopes a standard specimen USGS24 (δ13C = -16.0‰ vs. VPDB, IAEA, Austria, Vienna) was used.

Raman microspectroscopy studies of carbonaceous material, chemically extracted from microquartzites, were conducted in the Institute of Geology Karelian Research Center using Dispersive Raman Spectrometer Nicolet Almega XP (Thermo Scientific), and in the Center for Optical and Laser Materials Research of St. Petersburg State University on SENTERRA Express-Raman spectrometer Bruker, Germany).

2 GEOLOGY OF THE HOGLAND ISLAND

Hogland Island is located in the Gulf of Finland (Baltic Sea) on the southern margin of Baltic shield and Wiborg rapakivi granite batholith (WB). The metamorphic gneisses and amphibolites of Svecofennian basement (2 000 Ma), orogenic gabbrodiorites (1 950-1 900 Ma), post-orogenic granites and pegmatites (1 800-1 750 Ma) are outcropping in the western part of the island. They are overlain (in the eastern part of the island) by the subhorizontal strata of Hogland lithostratigraphic formation (HLF), presented by quartz conglomerate (thickness 0-20 m), basalts (0-40 m) and rhyolites (up to 110 m) (Figs. 1.1-1.3).

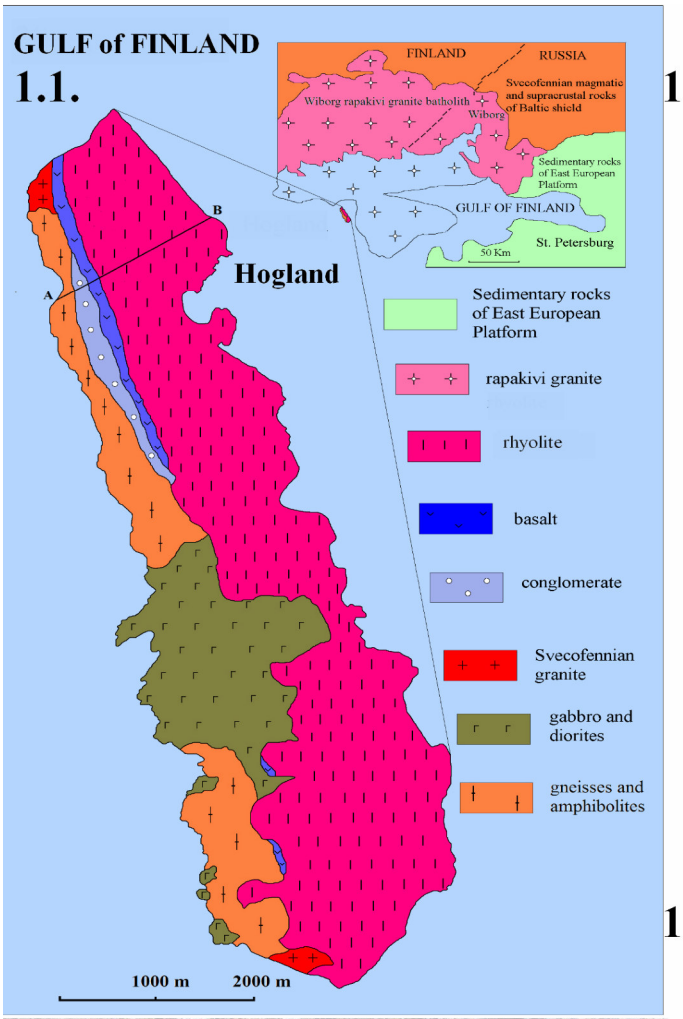
GULF of FINLAND
1.1.
FINLAND
RUSSIA
Wiborg rapakivi granite batholith
Wiborg
Svecofennian magmatic and supracrustal rocks of Baltic shield
Sedimentary rocks of East European Platform
GULF OF FINLAND
St. Petersburg
50 Km
B
A
Hogland
Sedimentary rocks of East European Platform
rapakivi granite
rhyolite
basalt
conglomerate
Svecofennian granite
gabbro and diorites
gneisses and amphibolites
1000 m
2000 m

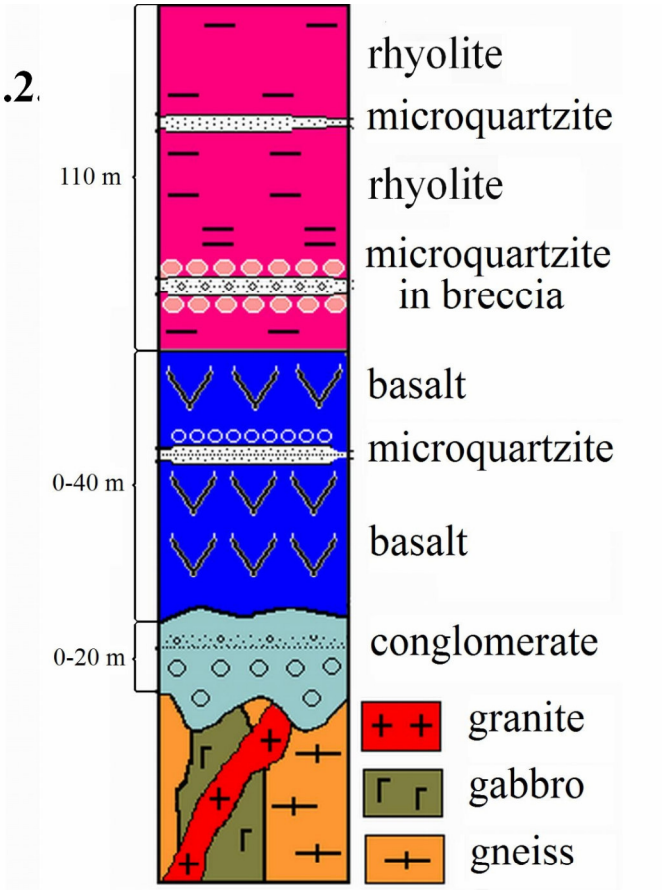
1.2.
110 m
0-40 m
0-20 m
rhyolite
microquartzite
rhyolite
microquartzite in breccia
basalt
microquartzite
basalt
conglomerate
granite
gabbro
gneiss

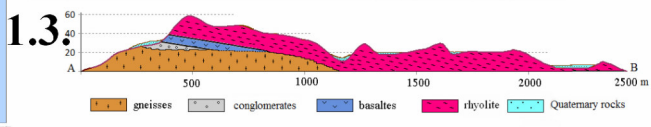
1.3.
60
40
20
A
B
500
1000
1500
2000
2500 m
gneisses
conglomerates
basaltes
rhyolite
Quaternary rocks

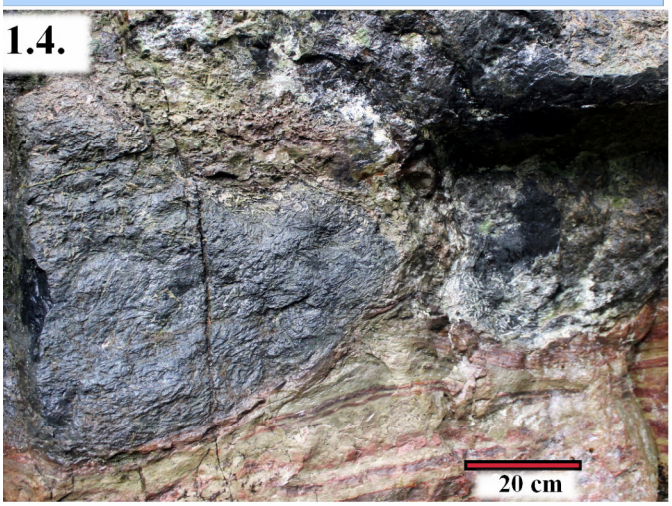
1.4.
20 cm

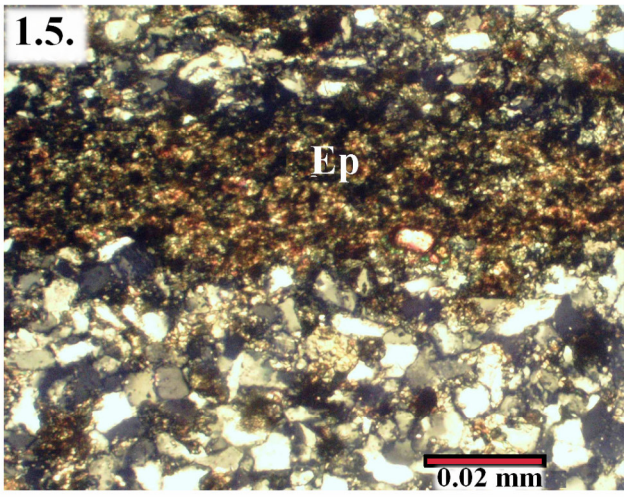
1.5.
Ep
0.02 mm


1.6.
Mk
20 cm

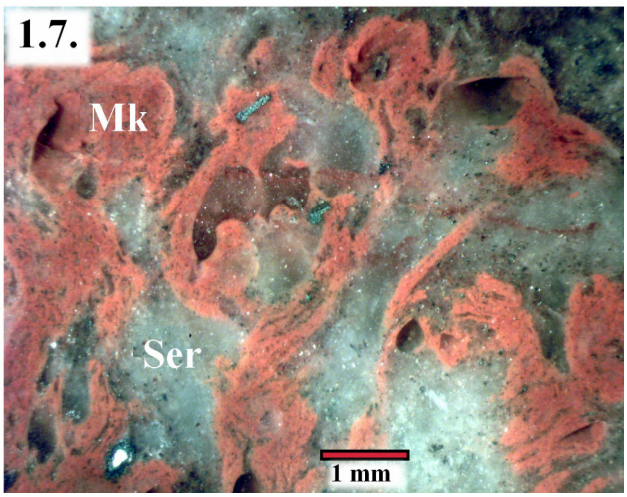
1.7.
Mk
Ser
1 mm

Figure 1. Geology and rocks of the Hogland Island. 1.1. Schematic geologic map of the Hogland Island. 1.2. Stratigraphic chart of Hogland lithostratigraphic formation. 1.3. Schematic geologic section of the Hogland Island on line A-B. 1.4. Basalt pillow laves overlapping strata of banded microquartzites. 1.5. Microstructure of banded microquartzites from basalt: dark grey interbeds are enriching small grain of epidote. Thin polished section with analyzer. 1.6. Pyroclastic breccia in rhyolites is cemented by microquartzites. 1.7. Cement of breccia in rhyolites: microquartzite (pink) and sericite aggregate (grey). Polished specimen.

2.1 Basaltic Lavas

Basaltic lavas form subhorizontal strata with pillow structures, which are typical for submarine volcanism. It contains subhorizontal lenticular bodies of metasedimentary finegrained microquartzites with banded textures, also formed in submarine conditions (Figs. 1.4‑1.5). Petrochemically, the basalts, trachybasalts and tephrites (on TAS classification diagram)−based on distribution of rare earth elements (REE patterns) and isotopic geochemical data (εNd(t)=-1.8, t=1 640 Ma)−are syngenetic to the gabbro-anorthosites of WB (Belyaev, 2013; Rämö et al., 2007; Belyaev et al., 1998, 1996; Rämö, 1991). However, the basalts have exceptionally extreme variations in the contents of Na2O (0.15 wt.%‑5.5 wt.%) and K2O (1.3 wt.%‑4.7 wt.%). In this case K2O/Na2O-ratio for these rocks varies from 0.3 to 20 (Table 1). The thin sections show intensive sericitization of the plagioclase blades in the margin zones of the basalt pillow structures. Basalts in this zone are enriched with K2O (3 wt.%‑4 wt.%) and depleted of Na2O (2.8 wt.%‑3.8 wt.%) as compared to the central sections of pillow structures (K2O 1.3 wt.%‑1.8 wt.% and Na2O 3.9 wt.%‑5.5 wt.%) (Table 1).

Tabl. 1. Chemical composition of basalts' and different parts of pillow structures

samples	Basalts' of lower strata			Basalts' of upper strata			pillow structure – 100 cm		pillow structure – 60 cm	
							centre	margin	centre	margin
oxides wt%	B1605	B1605	B1810	B1805	B1806	B1808	B1908	B1907	B1907c	B1907k
SiO_2	51.2	49.61	45.62	48.68	48.06	47.35	49.4	44.6	50.6	47.8
TiO_2	3.1	3.24	2.9	2.54	2.48	2.62	3.2	2.6	2.3	2.5
Al_2O_3	13.19	13.09	14.79	17.87	18.26	17.93	15.6	18.3	18.6	17.7
Fe_2O_3	15.98	14.69	7.74	5.76	8.35	7.37	9.0	7.5	7.1	6.8
FeO	0.01	0.01	8.47	6.65	3.36	3.92	5.0	4.0	3.7	4.3
MnO	0.18	0.16	0.18	0.11	0.1	0.14	0.09	0.18	0.1	0.15
MgO	3.13	3.14	5.81	2.14	1.83	4.67	3.3	5.8	3.0	5.5
CaO	7.9	10.42	7.85	7.34	7.51	4.95	6.6	7.3	4.8	5.5
Na_2O	0.87	0.33	0.15	2.83	3.54	4.03	3.9	2.8	5.5	3.8
K_2O	2.63	3.6	3.05	3.15	3.36	4.06	1.3	4.1	1.8	3.1
P_2O_5	0.71	0.69	1.0	0.93	0.92	0.81	0.92	0.75	0.71	0.75
H_2O	1.2	1.2	2.57	1.63	2.21	1.64	1.8	2.0	1.9	2.1
Total	100.1	100.18	100.13	99.63	99.99	99.49	99.19	99.18	99.4	99.25
K_2O/Na_2O	3	11	20	1.1	0.95	1.0	0.3	1.5	0.3	0.8

We assume that such intensive variations in chemical composition were caused by interaction of basaltic magmas with hot seawater enriched with K. The changes of the chemistry of basaltic lavas caused by interaction with Na-enriched seawater (hydrothermal albitization of basalt, or spilitization) were studied for modern and ancient submarine volcanism (Frikh-Khar, 1982). However, in both basic and acid volcanic rocks of the Wiborg Massif, the interaction with water during underwater eruption was accompanied by leaching of sodium and addition of potassium, expressed as sericitization of devitrificated groundmass and blades of plagioclase. Therefore, we can assume that in this case the water heated by lava pools was enriched with potassium.

2.2 Rhyolites

The rhyolites of Hogland form subhorizontal strata (in some areas over 110 m thick), overlaying the basalts. Pillowlike structures were found in rhyolites formed in submarine conditions. There are the subhorizontal lenticular strata (thickness 5‑20 cm) of sedimentary microquartzites in rhyolites, and pyroclastic breccias with microquartzite cement (Figs. 1.6.‑1.7.). This provides additional evidence of submarine volcanism conditions. The petrochemical features, REE patterns, isotopic, and geochemical characteristics of rhyolites (U-Pb age of zircons 1 640±11 and 1 638 ▪ 4 Ma), (εNd(t)= -1±0.5, t=1 640 Ma) are similar to the ovoid-bearing rapakivi granites of 1.64 Ga WB (Belyaev, 2013; Rämö et al., 2007; Belyaev et al., 1998, 1996; Rämö, 1991). Our data confirm that rhyolites are syngenetic to WB rapakivi granites. However, phenocrysts of orthoclase and devitrificational glass of the groundmass in rhyolites are highly sericitized, creating unique ratio of alkalis: high contents of K2O (6.9 wt.%‑9.3 wt.%) and relatively low content of Na2O (0.2 wt.%‑0.75 wt.%). Therefore, their K2O/Na2O-ratio varies from 10 to 47, while in WB rapakivi granites this ratio varies from 2 to 2.2 (Table 2).

Tabl. 2. Chemical composition of rhyolites

Samples oxides wt%	B1601	B1603	B1606	B1913	B1909
SiO_2	70.06	73.69	69.76	69.00	70.5
TiO_2	0.37	0.36	0.39	0.33	0.38
Al_2O_3	13.75	14.01	14.72	13.2	13.4
Fe_2O_3	4.59	3.15	2.56	3.1	3.1
FeO	0.01	0.01	1.89	1.2	1.2
MnO	0.02	0.02	0.05	0.22	0.01
MgO	0.16	0.29	0.26	0.26	0.63
CaO	1.62	0.87	1.73	1.7	1.2
Na_2O	0.57	0.18	0.15	0.42	0.79
K_2O	8.28	6.59	7.11	9.3	7.7
P_2O_5	0.03	0.03	0.01	0.11	0.13
H_2O	0.9	1.1	1.37	0.94	0.84
Total	100.36	100.31	100.0	99.78	99.88
K_2O/Na_2O	14.5	36.6	47.4	22.1	9.7

High content of K2O and relatively low content of Na2O in rhyolites are interpreted here as a consequence of hydrothermal interaction of eruptive rapakivi granite magmas with Paleoproterozoic Underwater Volcanism and Microfossil-Like Structures in the Metasedimentary Siliceous Rocks hot seawater enriched with K. Thus, we assume that abnormal alkali ratios in rhyolites and basalts, together with field evidence, such as presence of pillow-like structures, result from hydrothermal interaction of sea water with magma. Our data suggest that potassiumenriched hydrotherms were formed under the influence of K content plutonic fluids mixing with the seawater. These hydrothermal fluids could derive from alkaline basalts and rapakivigranite magmas, and could enrich the seawater with potassium before eruption.

2.3 Petrology of Siliceous Metasedimentary Rocks—Microquartzites

Subhorizontal lenticular strata of fine-textured quartzites (0.1–2 m in thickness) are found among flows of basalt and rhyolite lavas. Inside the strata of rhyolites in the crust of lava flows there are interlayers of eruptive breccias cemented by microquartzites and fine-grained sericite aggregate (Figs. 1.4., 1.5., 1.6., 1.7.). The environment of microquartzite formation can be reconstructed using geological and geochemical data: the nearbottom seawater was heated to high temperatures by very hot basalt and rhyolite lavas. Hot water dissolved the siliceous material on the surface of the flows. Silicon oxide solubility in the seawater decreased sharply in the upper layers of the sea basin. Consequently, chemogenic silicon-containing sediments were deposited on the surface of lava flows. They underwent contact metamorphism of albite-epidote-hornfels facies and turned into microquartzites due to heat and pressure created by the overburden lava flows.

2.3.1 Microquartzites in basalts

Microquartzites in basalts form subhorizontal lenticular strata within the flows and encircle basalt pillows-structures. They have banded structures created by interbedding of light grey and dark grey strata (Figs. 1.4, 1.5, Table 3).

Tabl 3. Chemical composition of microquartzites from basalts' and cement breccias in rhyolites in wt%

	microquartzites from basalt's				microquartzites from rhyolites		
Samples	B1906	B-1906-1	B1807	B-1809-1	B1602	B1604	B1604-1
oxides wt%							
SiO_2	78.6	77.8	76.43	83.3	78.92	80.8	87.8
TiO_2	0.38	0.45	0.53	0.22	0.36	0.24	0.57
Al_2O_3	8.0	9.01	8.49	4.98	10.49	7.38	5.8
Fe_2O_3	2.2	3.01	2.83	5.23	4.17	2.79	1.4
FeO	0.47	0.02	0.49	0.02	0.02	0.28	0.71
MnO	0.02	0.04	0.04	0.11	0.02	0.04	0.01
MgO	1.4	0.73	1.74	0.9	0.29	0.64	0.42
CaO	3.8	3.48	4.01	2.6	0.54	3.25	0.18
Na_2O	0.15	0.36	0.15	0.62	0.21	0.15	0.15
K_2O	3.7	4.5	3.87	1.76	4.14	3.37	1.6
P_2O_5	0.13	0.08	0.11	0.06	0.05	0.01	0.11
H_2O	0.78	0.82	0.99	0.48	0.9	1.02	0.97
Total	99.63	100	99.68	100	100.11	99.97	99.72

The mineral composition of microquartzites from basalts was determined in Saint Petersburg State University Resource Center using X-ray diffraction analysis on Bruker D2 Phaser Desktop powder diffractometer: quartz [SiO2]; microcline [KAlSi3O8]; albite [Na(AlSi3O8)]; biotite [(K0.84Na0.03)(Fe0.6Mg0.33Mn0.01)(Fe0.39Al0.27Mg0.28Ti0.06)2((Si2.71Al1.29)O10.25)(OH)1.68 F0.07]; calcite [CaCO3]; epidote [Ca2(Al,Fe)3(Si2O7)(SiO4)(OH)2].

The dark grey interbeds in microquartzites, as compared with the light grey strata, are enriched with small grains of epidote, possibly formed by recrystallization of sedimentary ash materials (volcanic glass particles) during contact metamorphism. Dark grey interbeds often have boudinage structures and are inPaleoproterozoic Underwater Volcanism and Microfossil-Like Structures in the Metasedimentary Siliceous Rocks tersected by thin veins of secondary epidote, which was crystallized in the later metasomatic process.

Isotope mass spectrometry studies of carbon-containing substance chemically extracted in microquartzites from basalts showed carbon vastly depleted of heavy isotope 13C (δ13C=-27.1‰– -27.3‰) (Table 4). This is typical for rocks formed with participation of living substance and confirms primitively submarine origin of microquartzites.

Tabl. 4. Carbon isotope composition (δ13CPDB, ‰) of graphite from microquartzites in basalts and rhyolites

materials	δ13C
carbon of graphite from microquartzites of basalt's	– 27.3
carbon of graphite from microquartzites of basalt's	– 27.1
carbon of graphite from microquartzites of rhyolites	– 29.5
carbon of graphite from cement breccias in rhyolites	– 28.9
Biogenic CO2	– 25 – –30

The Raman spectra of the remaining carbonaceous material chemically extracted from microquartzites in basalts contain bands indicating graphite: λG=1 579 cm-1; λD1=1 350 cm-1; λS2=2 700 cm-1 (Biske et al., 2015; Jehlička et al., 2003).

2.3.2 Microquartzites in rhyolites

Microquartzites in rhyolites, as well as in basalts, are primarily of sedimentary origin. They form lenticular strata within the rhyolite flows (thickness 0.1–0.3 m). Quartz, hematite and muscovite,

(K0.94Na0.04)(Al1.88Fe0.12Mg0.07Ti0.03)((Si3.01Al0.99)O10.11) (OH)1.85F0.04 predominate in the composition of cement of breccias. Additionally, there is fine-textural sericite (muscovite) aggregate associated with microquartzites in the cement of breccias in the rhyolites (Figs. 1.6, 1.7). The sericite aggregate could form from pelitic clay sediment recrystallized in contact metamorphism environment. Chemical composition of muscovite from the cement of breccias in the rhyolites was determined using JSM-6510LA raster electron microscope with JED-2200 energy dispersing spectrometer (JEOL, Japan): SiO2, 46.5 wt.%; TiO2, 0.55 wt.%; Al2O3, 36.37 wt.%; FeO, 4.32 wt.%; MnO, 0.06 wt.%; MgO, 0.16 wt.%; Na2O, 0.01 wt.%; K2O, 12.03 wt.%; total, 100 wt.%.

The Raman spectra of the remaining carbonaceous material chemically extracted from microquartzites in rhyolites contain bands indicating graphite: λG=1 572 cm-1; λD1=1 345 cm-1; λS2=2 700 cm-1 (Biske et al., 2015; Jehlička et al., 2003).

Isotopic composition of carbon (δ13CPDB= -28.9‰– -29.5‰, Table 4) in carbonaceous material of breccias' cement clearly indicates inflow of marine living substance during sedimentation. However, the sericite aggregate, theoretically, could have hydrothermal origin. Therefore, petrographic microscopic studies were carried out, which discovered four genetically different generations of quartz xenocrysts in the microquartzites and the sericite aggregate.

2.3.3 Generation of quartz xenocrysts in microquartzitesand sericite aggregate

The first generation of xenocrysts consists of fragments of equant quartz aggregates (size 0.5–1 mm) with serrated contact between grains and undulatory extinction of crystals (Fig. 2.1). This is typical for quartz grain aggregates of metamorphic gneisses, recrystallized under dynamic stress conditions (Fig. 2.2). The second generation of quartz xenocrysts consists of rounded globules (up to 0.3 mm in diameter), composed of finetexture quartz aggregate (Fig. 2.3). Quartz has undulatory extinction and serrated contacts between grains, typical for quartz grain aggregates from dinamometamorphic rocks (Fig. 2.4). The third generation of xenocrysts consists of rounded grains of quartz (0.5–1 mm in diameter) with uniform extinction, typical for phenocrystic quartz grains from rapakivi granites (Figs. 2.5, 2.6). The fourth generation of xenocrysts consists of large rounded grains of quartz (0.5–1 mm in size) with total or sectorial extinction of crystals. These grains have distinctive "gulfs"—dissolution cavities, typical for quartz grains from rhyolites (Figs. 2.7, 2.8). The presence of quartz grain xenocrysts from rocks of different genesis in the microquartzites and the sericite aggregate of breccias' cement from rhyolites indicates their sedimentary origin. Xenocrysts could get in the chemical siliceous and fine-dispersed pelitic sediments as a result of wind transfer by sandstorms.

3 MICROFOSSIL-LIKE STRUCTURES IN METASEDIMENTARY ROCKS

In the microquartzites among basalts, rhyolites and cement of breccias of rhyolites we discovered structures with external and internal morphology similar to modern or fossilized marine microorganisms. The structures similar to spiral cyanobacteria, amoebas, diatoms, foraminifers, virus capsids, flagellates and multicellular organisms were studied in polished samples and in thin transparent sections using both optical and scanning electron microscope. We believe that these structures are remains of microfossils representing the Paleoproterozoic community of marine microorganisms.

3.1 Spiral Cyanobacteria

Microfossils of cyanobacteria are known in Archean and Paleoproterosoic rocks (Rozanov and Astafieva, 2009; Rozanov, 2002). Spiral structures similar in morphology to microfossils of Spirulina cyanobacteria were observed in thin sections of microquartzites from basalt pillow lavas. External boundaries of these spiral structures consist of chains of hematite, epidote and chlorite grains. Raman microspectroscopy shows that the external boundaries of spiral structures contain of carbon material. The inside of the spiral structures consists of hematite, epidote, or microquartzites (Figs. 3.1–1.3).

The structures of microquartzites inside the spiral boundaries and in the enclosing groundmass are completely identical (Fig. 3.1, SS-2). This is typical for microfossil pseudomorphoses, with the same substance inside and outside of the specimen. Apparently, chemogenous siliceous gel (possibly isotropic opal) was inside and outside of the spiral structures, subsequently converted into microquartzites during contact metamorphism.

Hematite grains in the external boundaries of structures formed during recrystallization of iron hydrate adsorbed on the surface of the bacteria. Apparently, epidote and chlorite crystallized from hydrothermal solutions on the geochemical barriers from hematite and amorphous carbonic material.

3. 2. Amoeba-like Structures

The oldest microfossils of agglutinated amoeba shells are known in the Neoproterozoic rocks [26]. The objects found in microquartzites within basalts and rhyolites with high degree of probability can be considered amoeba-like structures. They have isometric or rounded exterior boundaries (up to 0.5–2 mm in diameter) composed by chain grains of hematite, epidote, chlorite and disordered (amorphous) carbonic material. Inside the boundaries the structures are filled with finer microquartzite (quartz grain size 5–10 μm), than the quartzite in the enclosing groundmass (grain size 10–40 μm) (Fig. 3.4).

In the microquartzites from one of the amoeba-like structures we found objects resembling spiral bacteria with hematite and epidote boundary and microquartzite inside (Fig. 3.5). It is possible that this object is the pseudomorphose on the relicts (residue) of substance of "hogged down" bacteria, "indigested" by amoeba-like organism.

Linear forms formed of chains of hematite grains were observed inside the amoeba-like structures in the cement of breccias from rhyolites. Possibly, they are ferruginized fragments of endoplasmic reticulum organelles, typical for modern eukaryotic organisms (Fig. 3.6).

Microquartzite inside amoeba-like structures could be a result of metamorphogenic recrystallization of silicified protoplasm, and the hematite grains in the external boundaries of structures grew during recrystallization of iron hydrate adsorbed on the surface of amoebas.

3. 3. Diatom-like Structures

The earliest known fossil diatoms (*Hemiaulus* and *Triceratium*) are from the early Jurassic (~185 Ma ago) [15], although these eukaryotes, undoubtedly, have earlier origin.

Structures similar by morphology to *Hemiaulus* and *Triceratium* diatoms occur in microquartzites within basalts and rhyolites (Fig. 3.7–3.9). Their boundaries resemble cups and triangles, formed by chains of small hematite or epidote grains, with microquartzite inside (Fig. 3.9).

3. 4. Foraminifera-like Structures

Foraminifera Microfossils are known in the rocks of Neoproterozoic and Cambrian [18]. We found structures with morphology similar to foraminifera in microquartzites within basalts and in the cement of breccias within rhyolites. They are shaped as rounded multicamerate shells with external boundaries consisting of chains of small hematite grains (Fig. 3.10–3.12). In the central parts of foraminifera-like structures, we observed partitions and rounded zonal nucleus-like object, composed of hematite (Fig. 3.11). Structures of microquartzites inside boundaries of foraminifera and in the enclosing groundmass are identical.

3. 5. Virus-like Structures

Viruses inhabit all contemporary ecosystems of the Earth [16], and, possibly, have existed since the appearance of the first living cells [11]. However, as of today, there are no findings of virus microfossils even in the contemporary deposits.

In the thin section of microquartzites from the basalts we observed boundaries of zonal hexahedral or pentahedral structures (Fig. 4.1) with morphology similar to icosahedral capsids of contemporary mimiviruses [11, 16].

The structure of microquartzites inside the boundaries and in the enclosing groundmass is identical (Fig. 4.1, Right). This evidences that the substance inside and outside of the zonal boundaries, which consisted of siliceous gel, was originally identical, as in the pseudomorphoses of microfossils with spiral and foraminifera-like structures. External and internal boundaries of zonal structures are composed of chains of small hematite grains, formed during metamorphic recrystallization of iron hydrate adsorbed on the surface of the virus-like cells.

We found fragments of zonal virus-like structures in the groundmass of microquartzites and at the contact with amoeba-like structures (Fig. 4.2). This resembles penetration of modern enveloped viruses

into the cell by merging with the cell membrane. In such cases, the remains of proteinaceous substance remain on the surface of the cell membrane.

In the cement of breccia from rhyolites we found hexahedral and pentahedral forms with external morphology similar to icosahedral capsids of contemporary mimiviruses (Fig. 4.3–4.8). They consist of quartz-hematite aggregate containing 10–30% hematite (Fig. 4.3–4.5 and 4.7–4.8) or microquartzites grains, coloured brown by iron oxides (Fig. 4.6). Quartz-hematite aggregate has specific symplectic texture of intergrowth of two mineral phases formed by crystallization of siliceous gel and iron hydrates (Fig. 4.7–4.8). Viruses-like structures in sericite aggregate are enclosed in microquartzite conches.

Therefore, the hexahedral or pentahedral structures in microquartzites of basalts and in the cement of breccias from rhyolites could be pseudomorphoses of virus-like microfossils.

3. 6. Flagellate-like Structures

Flagellate is a single-celled organism with one or more whip-like organelles, and a mantle filled with cytoplasm, nucleolus, vacuoles, sometimes covered with mucous pellicle. Ancient microfossils of *Dinoflagellate* cysts were found in the rocks of Triassic period.

Flagellate-like structures (provisionally named *Protoflagellate yukhalina*) are found in the microquartzites and the sericite aggregate of cement of breccia in the rhyolites together with quartz xenocrysts from dinamometamorphic rocks (Fig. 5.1, 5.2 and 5.6).

They have rounded forms (0.5–1 mm in size) and one or more whip-like offshoots. Inside the flagellate-like structures consist of microquartzites, coloured brown by iron oxides, or of quartz-hematite aggregate containing 10–30% hematite grains. Quartz-hematite aggregate has specific symplectic texture of intergrowth of two mineral phases formed by cristallization of siliceous gel and iron hydrates (Fig. 5.4–5.5). The FlS located in the sericite aggregate, together with whip-like offshoots, are surrounded by siliceous mantle, initially composed of opal, which replaced the external mucous pellicle of the cell.

In the central parts of the flagellate-like structures we observed rounded shapes similar to nuclei and vacuoles, composed of hematite-quartz aggregate or hematite (Fig 5.3, 5.5). Additionally, the cell is crossed by linear structure composed of hematite and bordered with quartz, with morphology similar to “aksostil” organelle (Fig 5.3).

3.7. Structures are similar to microfossils of multicellular micro-organism’s in sericite aggregate of cement breccia from rhyolites.

Organisms consisting of more than one cell are called multicellular. The first evidence of multicellularity is colonial organisms, which lived 2.1 billion years ago [9].

We observed objects similar to microfossils of multicellular microorganisms in thin sections and polished samples. They consist of several rounded forms composed of microquartzites inside and hematite-quartz aggregate outside (Fig 5.7–5.11). Sometimes multicellular structures with whip-like offshoots are bordered by siliceous covers (5.7, 5.9 and 5.10). Possibly, this is silicified mucous pellicle of the structures similar to zygotes or gametes (Fig. 5.7).

Thus, the following facts indicate that fossil-like objects in microquartzites from basalts and rhyolites are fossilized remains of ancient aquatic microorganisms:

1. Morphological likeness of these structures with modern or fossilized aquatic microorganisms.
2. A variety of fossils like structures and joint their association in space.
3. Identity of microquartzite structures in matrices and inside of the microfossils like objects.
4. The presence of the biogenic carbon in the microquartzites from basalts and rhyolites.

4. Discussion

Petrogenesis of Precambrian potassic alkaline volcanites spatially and temporally associated with rapakivi granites is one of the discussion problems of Petrology of magmatic complexes.

The original geochemical data and the presence of pillow structures in basalts and rhyolites of the island of Hogland clearly show that volcanic rocks during underwater eruptions interacted with sea water, rich in potassium. Interlayers in the volcanic suite of the metasedimentary siliceous rocks depleted in 13C, and interpreted here as evidence of ancient marine life confirms these data.

Potassic alkaline volcanites of Proterozoic age associated with rapakivi granites, also known in China, Finland, USA, Brazil. So, a suite Pinggu of potassic alkaline volcanites (K-phonolites) is known

in Proterozoic (1.85 to 1.40 Ga) rifting in the Beijing area, China [24]. «The suite is bimodal comprising high-potassic basaltic and phonolitic rocks and rapakivi granites» [13]. K-phonolite interbedded with trachybasalt, and covered by dolomite. «The characteristics of marine eruptions are not very obvious in the volcanites, possibly because they rapidly formed volcanic islands by quick accumulation» [13]. However volcanic cyclothems are separated by dolomite intercalations, which obviously have submarine origin. In this case trachybasalts have the high potassium content in the (K_2O = 2.1 to 8.2) and phonolites shows (K_2O 11.7 to 14.9 high). Therefore K_2O /Na_2O ratios change in limits = 6.9 to 33 [13].

Potassic alkaline volcanites of the Middlebrook group is known in Precambrian (1.48 to 1.45 Ga) in the St. Francois Mountains of southeastern Missouri Wisconsin, USA [14, 23]. They spatially and temporally associated with rapakivi granites and volcano-sedimentary rocks: ignimbrite, ash flow tuff, and water-laid tuff. Sometimes rhyolites have «local intensive alteration including silicification, potassium metasomatism, sericitization, and propylitization» [14]. These rhyolites shows considerable variation in content of Na_2O (0.12–2.68 wt. %) and the high potassium content (K_2O = 5.89 to 9.76), therefore K_2O/Na_2O ratios change in extraordinarily wide limits (2.2 up to 74). The presence in volcanites of high potassic rocks might indicate anomalous magma types [6, 14]. On the other hand, the high K_2O/Na_2O ratios in rhyolites may be result of laid K-metasomatic process [14].

Thus, it is possible to assume that the high content of potassium and extraordinary change of the K2O/Na2O relationships in volcanic rocks Pinggu and Middlebrook can also be the result of superimposed K-metasomatism processes in time of underwater eruption and interaction magmas with sea water enriched by potassium.

The siliceous rocks from siliceous volcanogenic complexes of Proterosoic and Phanerosoic formations have mostly sedimentary clastic origin and contain remains of microfossils already dead microorganisms with solid siliceous skeletons, predominantly of radiolarian and diatoms [10]. However, siliceous chemical sedimentary rocks preserve microfossils without solid mineral skeleton better. Studies of silification of cyanobacteria near contemporary thermal springs [1, 21, 22], and experimental dates [5] showed that these processes occur in even living organisms very quickly, within few hours. Microfossils virus is not found even in modern sediments, but there is evidence of experimental fossilization of viruses from extremophilic Archaea: «Our results confirm that viruses can be fossilised, with silica precipitating on the different viral structures (proteins, envelope) over several months in a manner similar to that of other experimentally and naturally fossilised microorganisms. This study thus suggests that viral remains or traces could be preserved in the rock record although their identification may be challenging due to the small size of the viral particles» [17]. However, ancient viruses could have a huge size and exceed the most modern large mimivirus a thousand times (like the dinosaurs in the class of reptiles).

Hot seawater saturated with silicon oxide and iron (during underwater volcanism) was favourable for quick fossilization – silification and ferruginization of marine microorganisms without solid mineral skeleton. Hot solutions infused still living cells and led to replacement of intracellular cytoplasm by siliceous gel (opal or chalcedony). Iron hydrate deposited on the surface of cell membranes, partitions and organelles. Microquartzites and quartz-hematite aggregate with specific symplectic texture of intergrowth of two mineral phases – quartz and hematite – formed in the process of metamorphic recrystallization.

The features of metasedimentary rock structures depend on the formation environment – initial chemical composition of sediments, physical properties of fractions and parameters of metamorphic transformation (temperature, pressure, number of crystallization centres). Therefore, the identity of microquartzite structures in the matrix of the rock and inside microfossil-like structures suggests identic formation environment. The epidote and chlorite of the internal and external boundaries of structures apparently crystallized from hematite and carbonaceous material in hydrothermal solutions at geochemical barriers.

The concentrations of biologically scarce elements of potassium and phosphorus in seawater limit the abundance and diversity of life. Therefore, considerably elevated potassium concentration in seawater of the Abel Sea could be beneficial to the evolutionary development of microorganisms.

Moreover, 90–98% of seawater radioactivity is caused by the radioactive isotope ^{40}K (half-life $T_{½}$ = $1.3 \cdot 10^9$ Ga). Consequently, 1.64 billion years ago the content of ^{40}K in a natural mixture of isotopes was approximately 2.3 times more than at present. Therefore, given the overall high potassium concentration

in the seawater, background radiation at that time exceeded the modern level more than 10 times. In this case, ^{40}K concentrated inside the cells in the immediate vicinity of DNA and its radioactivity caused spontaneous mutagenesis, necessary for evolutionary development, selection and new speciation.

Phosphorus is also an important biophile element, essential for the synthesis of proteins. The concentrations of phosphorus in the water limit the growth of microorganisms. Basalt is the rock supplying the most phosphorus to the seawater (Clarke value P – 0.14%). Content of phosphorus in the basalt of Hogland is wary high – 0.69–1% P_2O_5 (0.39–0.56% P) (Table 1).

High concentrations of biologically scarce elements potassium and phosphorus in the Sea waters and high radioactivity of the environment and inside the microorganisms were favourable for their evolutionary development.

5. Conclusions

During the underwater eruption of basaltic and rhyolitic lavas associated with the formation of the Wiborg rapakivi batholith, the seawater was saturated with silicon oxide. This led to formation of chemogenic silicate sediments and fast silification of living planktonic microorganisms. In this case, hydroxides of iron deposited on the surface of biological membranes and organelles. Sometimes the endoplasm was replaced by mixture of silicon oxide and hydroxides of iron. The fossilized planktonic microorganisms submerged in silicate sediments, which were transformed into microquartzites during contact metamorphism. In the local areas with the minimum lithostatic stress the morphology structures of microfossils were not significantly disturbed. This is especially important for well-preserved silificated and ferruginous microfossils recently found in the strata of the Proterozoic meta-siliceous rocks.

ACKNOWLEDGEMENTS

The would like to thank my colleagues for technical support: Belyaev G.M., Belyaeva N.V., Biske N.S., Bogdanov Y.B., Chistyakov K.V., Fedorov P.V., Filippov M.M., Galankina O.L., Kholmyanskii M.A., Kobilkov S.V., Kolodey V.A., Koltsov A.B., Mazalova E.A., Platonova N.V., Polekhovski Y.S., Prasolov E.M., Putinseva L.V., Shebanov A.D., Tabuns E.V., Yrchenko Y.Y., as well as for helpful discussions and comments on the manuscript: Krivovichev V.G., Podlipski I.I., Popov A.V., Zelenkovski P.S.

Special thanks to Yukhalin P.V., General Director of Sidose LLC, and Yukhalin E.P., for participation in the fieldworks and financial support of field trips, and too the Russian Geographical Society of the St. Petersburg.

In addition, a thank you to Alexander Alexandrov of Ardis Translation, who kindly proofread the English version of this paper.

This work was supported in part by grant from International Science Foundation [ISF, NY, USA] N RI E000, and grants of Russian Foundation for Basic Research (RFBR): № 95-05-15305, № 97-05-65446, and № 3.15.865.2013

REFERENCES

1. Bacterial paleontology, 2002, (red. Rozanov A.Yu), Moscow, PIN RAN, 88 p. (in Russia).
2. Belyaev A.M., Bogdanov Y.B., Levchenkov O.A., et al., 1996. Bimodal volcanic formations of the Wiborg batholith on the Island of Hogland (Suursaari), Russia // In: Rapakivi Granites and Related Rocks: Correlation on a Global Scale (Abstr. Vol. IGCP-315 Symp.), Helsinki, Finland, P. 5.
3. Belyaev A.M., Bogdanov Y.B., Levchenkov O.A. 1998. Petrogenesis of the bimodal rapakivi-related volcanites of the Island of Hogland, 1.64 Ga Wiborg batholith, Russia // In: Rapakivi Granites and Related Rocks: Correlation on a Global Scale (Abstr. Vol. IGCP-315 Symp.), Madison, USA, p. 139–140.
4. Belyaev A.M. Petrology of volcanic rocks from the rapakivi formation (Island Hogland) 2013. J. Regional Geology and Metallogeny, St. Petersburg, Russia, N 55. P. 28–36 (in Russia).
5. Benning L.G., Phoenix V., Yee M.J., et al. 2002. Molecular characterization of cyanobacterial cells during silicification: A synchrotronbased infrared study // Geochem. Earth Surf. Vol. 6. P. 259–263.

6. Bickford, M. E., J. R.Sides, and R. L.Cullers, 1981. Chemical evolution of magmas in the Proterozoic terrane of the St. Francois Mountains, southeastern Missouri, 1, Field, Petrographic, and major element data, J. Geophys. Res., v. 86 (B11) p. 10365-10386.
7. Biske N.S., Belyaev A.M., Kolodey V.A., 2015. Raman spectrum of carbonaceous material from hornstones of the Island of Hogland (Russia) // XII General Meeting of the Russian Mineralogical Society, St. Petersburg, Russia, P. 185–186 (in Russia).
8. Frikh-Khar D. I. 1982. The interaction of seawater with igneous matter. Soviet Geology, № 10. P. 93–99 (in Russia).
9. Grosberg R.K., Strathmann R.R., 2007. The evolution of multicellularity: A minor major transition? // Annu Rev. Ecol. Evol. Syst. Vol. 38. P. 621–654.
10. Filippov A.N., Kemkin I.V., 2009. Siliceous–Volcanogenic Complexes of Western Sikhote Alin: Their Stratigraphy and Origin // Russian Journal of Pacific Geology, Vol. 3, N 2. P. 154–167.
11. Iyer L.M., Balaji S., Koonin E.V., et al. 2006. Evolutionary genomics of nucleo-cytoplasmic large DNA viruses. Virus Res.; 117(1):156–84.
12. Jehlicka J., 2003. Raman spectroscopy of carbon and solid bitumens in sedimentary and metamorphic rocks // Spectrochimica Acta Part A: Molecular and Biomolecular Spectroscopy. Vol. 59, Issue 10. P. 2341–2352.
13. J. Yu, H. Fu, F. Zhang, and F. Wan. 1994. Petrogenesis of Potassic Alkaline Volcanics Associated with Rapakivi Granites in the Proterozoic Rift of Beijing, China. Mineralogy and Petrology. p. 83-96.
14. Kisvarsanyi E.B., 1972. Petrochemistry of Precambrian igneous province, St. Francois Mountains, Missouri. Report of Investigations, № 51. Rolla, Missouri, USA, 97 p.
15. Kooistra, W. H. C. F.; Medlin, L. K., 1996. Evolution of the Diatoms (Bacillariophyta) IV A Reconstruction of Their Age from Small Subunit rRNA Coding Regions and the Fossil Record. *Molecular Phylogenetics and Evolution* (Academic Press) 6 (3), p. 391–407.
16. Lawrence CM, Menon S, Eilers BJ, et al. 2009. Structural and functional studies of archaeal viruses. J. Biol. Chem. 284(19), p. 12599–603.
17. Orange, F.; Chabin, A.; Gorlas, A., et al. 2011. Experimental fossilisation of viruses from extremophilic Archaea, Biogeosciences, Volume 8, Issue 6, p.1465-1475
18. Pawlowski, J., M. Holzmann, C. Berney, J., et al. 2003. The evolution of early Foraminifera. Proceedings of the National Academy of Science, 100, p. 11494–11498.
19. Rämö O.T., 1991. Petrogenesis of the Proterozoic rapakivi granites and related basic rocks of southeastern Fennoscandia: Nd and Pb isotopic and general geochemical constraints // Geol. Surv. Finland, Bull. 155. p.
20. Rämö, O.T., Mänttäri, I., Huhma, H., et al. 2007. 1635 Ma bimodal volcanism associated with the Wiborg rapakivi batholith (Suursaari, Gulf of Finland, Russia). Sixth Hutton Symposium on the Origin of Granitic Rocks, p. 174–175.
21. Renaux K.O., Jones B., 1998. Tiercelin Rapid in situ silicification of microbs at Loburu hot springs, Lake Bogoria, Kenya Rift Valley // Sedimentology. V. 45. N 6. P. 1083–1103.
22. Rozanov A. Yu., Astafieva M. M., 2009. The Evolution of the Early Precambrian Geobiological Systems // Paleontological Journal. V. 43. N 8, p. 61–77.
23. Sides J. Ronald; Bickford M. E.; Shuster R. D.; Nusbaum R. L., 1981. Calderas in the Precambrian terrane of the St. Francois Mountains, southeastern Missouri. Journal of Geophysical Research, v. 86, p. 10349-10364.
24. Shuan-Hong Zhang, Shu-Wen Liu, Yue Zhao, et al. 2007. The 1.75–1.68 Ga anorthosite-mangerite-alkali granitoid-rapakivi granite suite from the northern North China Craton: Magmatism related to a Paleoproterozoic orogen. Prec. Res. V. 155, p. 287–312
25. Streng M., E. Babcock, and j. S. Hollingsworth, 2005. Agglutinated protists from the lower Cambrian of Nevada // J. Paleont., 79(6), P. 1214–1218.
26. Westall F., Boni L., Guerzoni E., 1995. The experimental silicification of microorganisms //J. Paleontol. V. 38(3), p. 495–528.

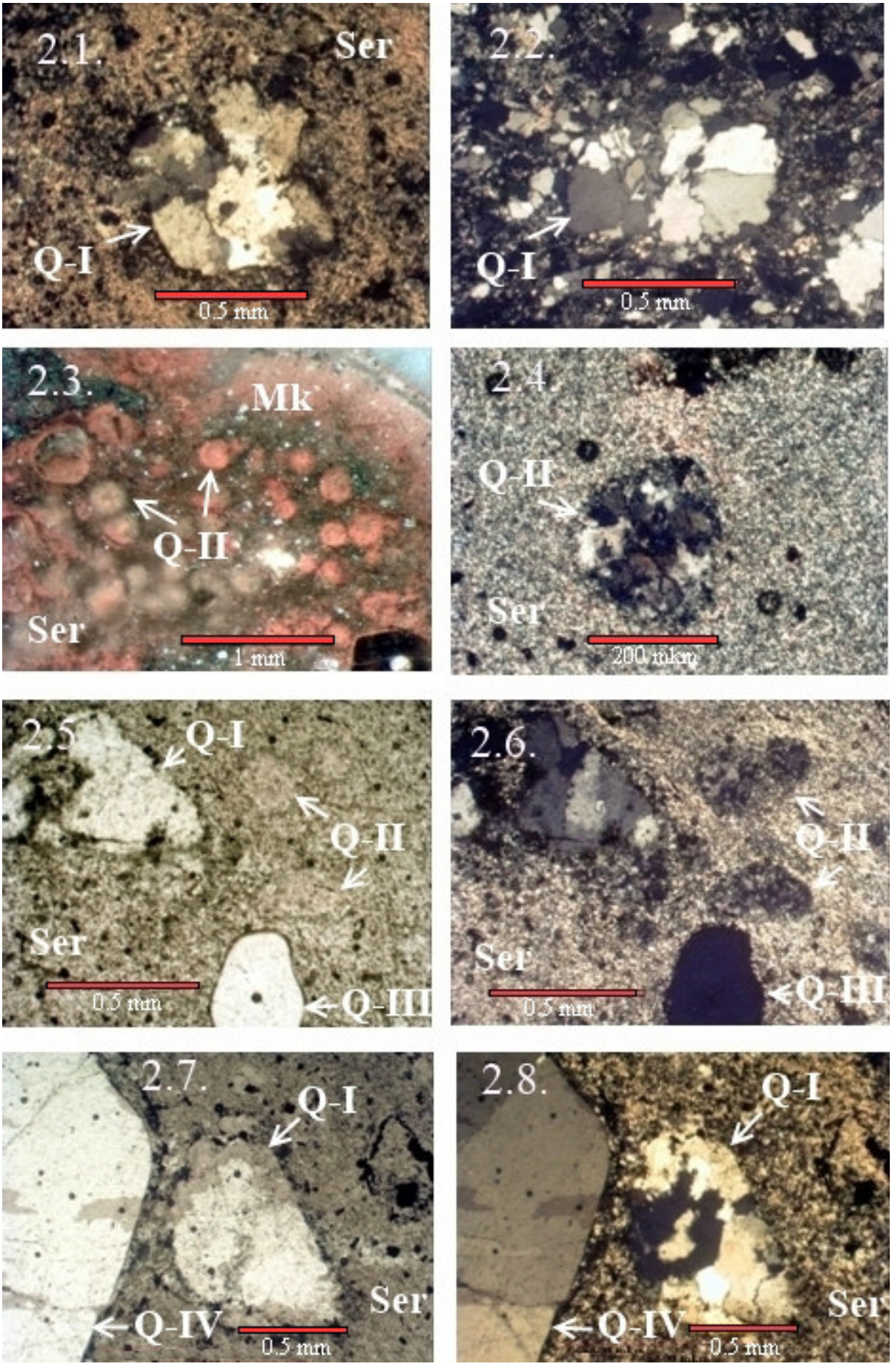

Figure 2: Generation of quartz in microquartzites and sericite aggregate from cement breccias in rhyolites:

2.1. The first generation of quartz xenocrysts with undulatory extinction and serrated contact between grains. Thin section, with analizer.
2.2. Aggregate of quartz grains with undulatory extinction and serrate contact between grains from gneisses of Hogland suite basement. Thin section, with analizer.
2.3. The rounded globules of quartz intergrowth of the second generation of xenocrysts in microquartzites (pink) and sericite aggregate (grey). Polished specimen.
2.4. The rounded globules of tin granular quartz intergrowth in sericite aggregate. Grain quartz has undulatory extinction and serrate contact between grains. Thin section, with analizer.
2.5. The first, second and third generations of quartz xenocrysts in sericite aggregate. A roundish quartz grain of third generation has total extinction, which are like quartz grains from rapakivi granites. Thin section, without analizer.
2.6. The same thing, as 5, with analyzer.
2.7. First and fourth generations of quartz xenocrysts in sericite aggregate. Fourth generation quartz grains have total or sectoral extinction of crystals, which is similar quartz grains from rhyolites. Thin section, without analyzer.
2.8. The same thing, as 7, with analyzer.

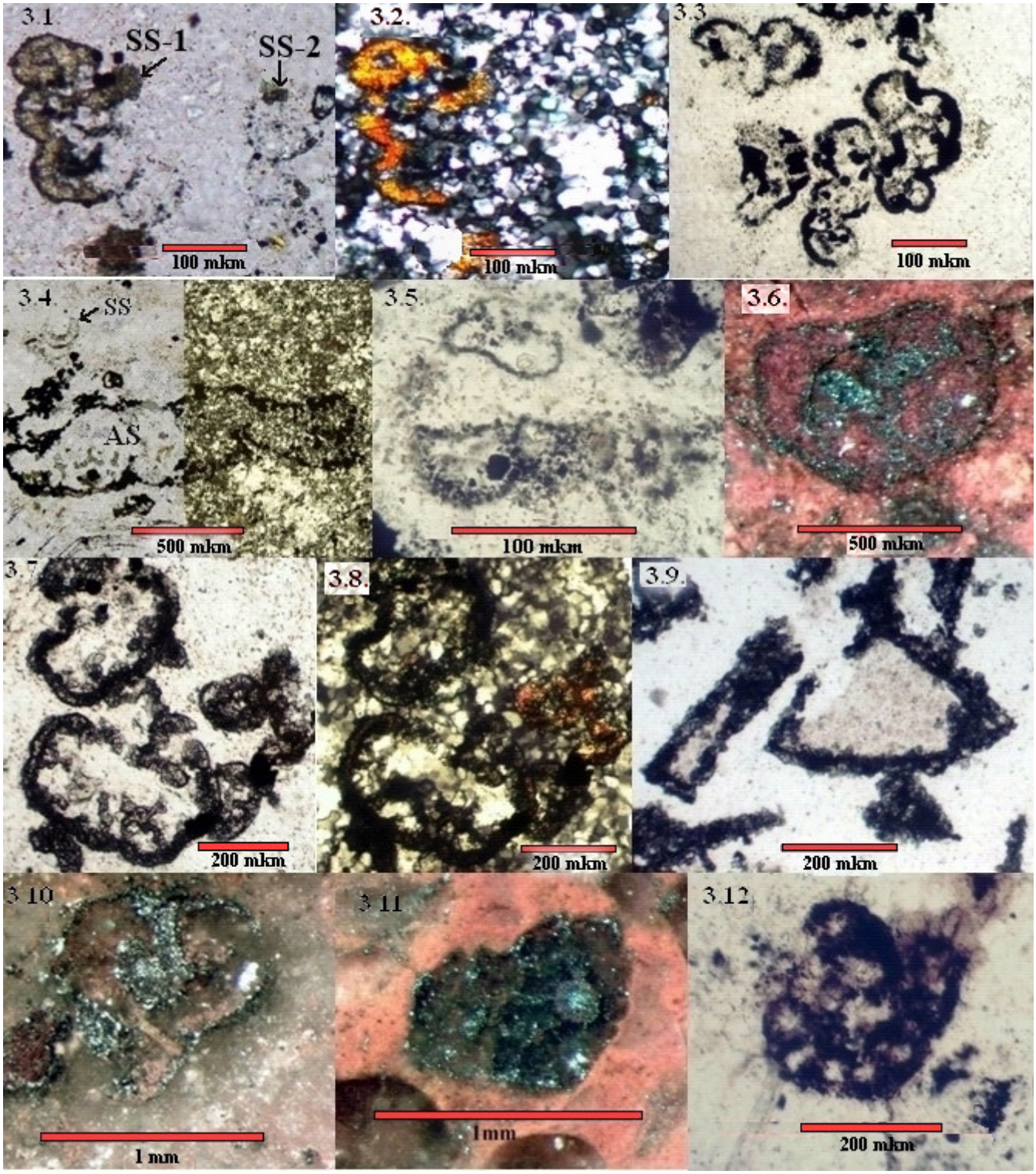

Figure 3. Assemblages of the microfossils like structures in microquartzites from the basalts and cement of breccias in rhyolites

3.1-3.3. Spiral structures (SS) in microquartzites from the basalts in the thin sections.

3.1. SS-1 – haematite in the external contour and the aggregates of epidote grains inside. SS-2 – hematite at the outer boundary, microquartzite inside. Thin section, without the analyzer.

3.2. Same as 1.1. with the analyzer.

3.3. SS – haematite in the external contour, and microquartzite in the internal, without the analyzer.

3.4-3.6. Amoeba like structures (AS) in microquartzites

3.4. AS in microquartzites from the basalts. The external contours are composed by the chains of grains of haematite, epidote and chlorite, internal by microquartzites with fine-texture. Thin section, left half without the analyzer, right half with the analyzer.

3.5. Fragment of SS inside the contour AS. Thin section, with the analyzer.
3.6. AS in the microquartzites from the cement of breccias in the rhyolites. The external contours are composed by chains of grains of haematite. Inside the boundary – microquartzite colored brown by iron oxides. Polished specimen.

3.7-3.9. Diatoms like structures (DS) in microquartzites in the thin sections.

3.7. DS of *Hemiaulus* genus in microquartzites from the basalts: the outer boundaries consist of hematite and epidote grain chains, the structure of microquartzites inside diatoms and in the groundmass are identical. Without analyzer.
3.8. The same, as 1.1., with the analyzer.
3.9. DS of *Triceratium* genus in microquartzites from the rhyolites. The outer boundaries consist of hematite and epidote, microquartzites inside. Without analyzer.

3.10.-3.12. Foraminifera like structures (FoS) in microquartzites

3.10. FoS in microquartzites from the cement of breccias in the rhyolites. The outer boundaries consist of hematite, microquartzites inside. Polished specimen.
3.11. FoS in microquartzites from the cement of breccias in the rhyolites. The outer boundaries, internal partitions and zonal rounded nucleus consist of hematite, microquartzites inside. Polished specimen.
3.12. FoS in microquartzites from basalts. The outer boundaries consist of hematite, microquartzites inside. Without analyzer.

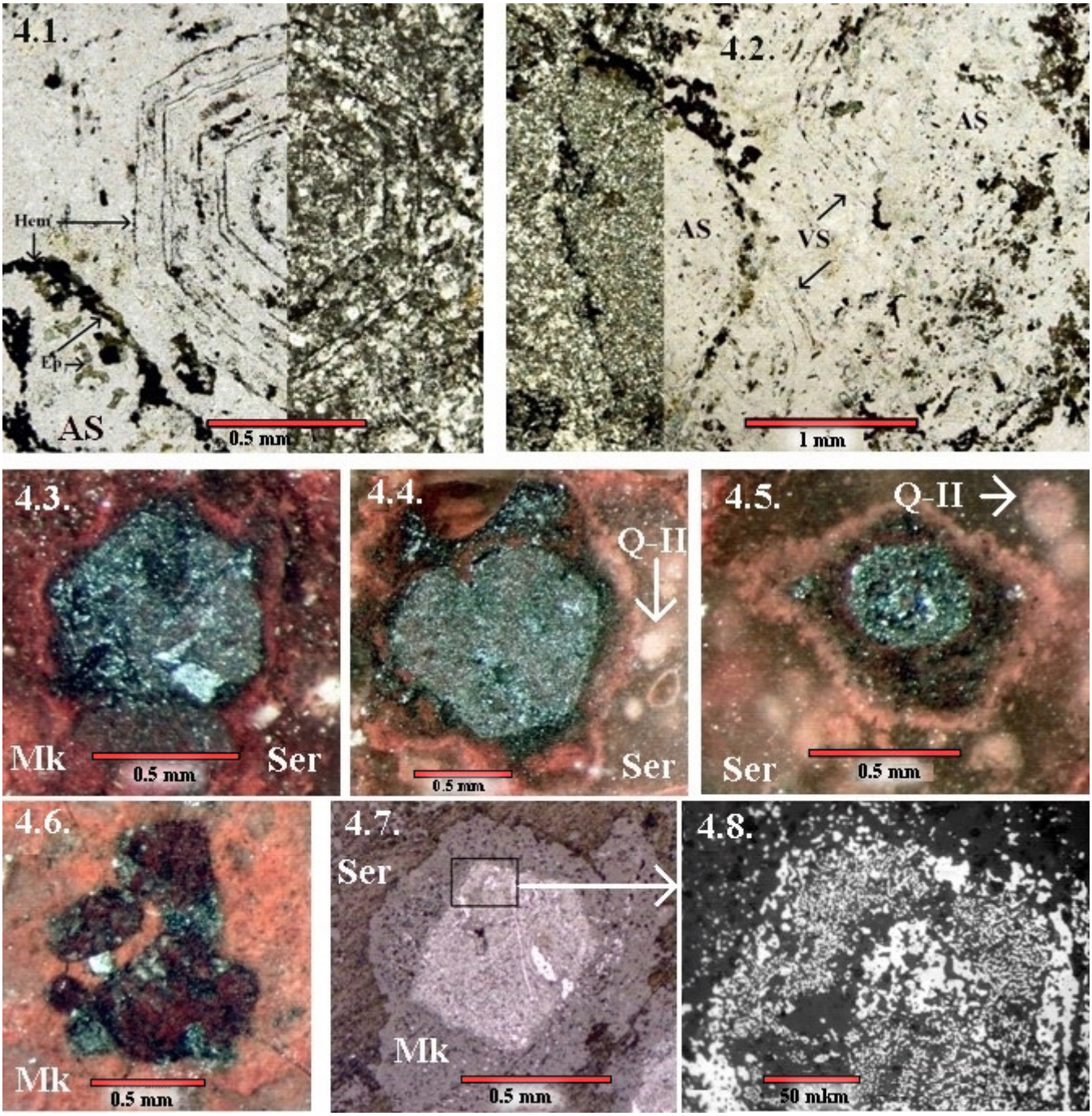

Fig. 4. Virus like structures (VS) in microquartzites from basalts (MB) (4.1.–4.2.) and from the cement of breccias in the rhyolites (4.3.–4.8.).

4.1. Left**.** Zonal hexahedral virus-like structure in MB with external and internal boundaries formed by chains of hematite grains. AS – fragment of the amoeba-like structure. Hem – hematite, Ep – epidote. Without analyzer. Right**.** Structures of microquartzites inside the **VS** boundary and in the groundmass are identical. With analyzer.

4.2. Fragments of the boundaries of zonal virus-like structures (VS) contacting with amoeba-like structures (AS). Left – with analyzer, right – without analyzer.

4.3.-4.8. VS consisting of quartz-hematite aggregate in sericite aggregate (Ser) and in microquartzites (Mk) from the cement of breccias in rhyolites.

4.3.-4.4. Hexahedral VS with Mk mantle. Q-II – quartz globules in Ser. Without analyzer.

4.5. Pentahedral zonal VS in Ser, with Mk mantle. Q-II – quartz globules in Ser. Without analyzer.

4.6. Two pentahedral VS in Mk consisting of microquartzites. Without analyzer.

4.7. Pentahedral VS in Ser, with Mk mantle. With analyzer.

4.8. Fragment of pentahedral VS (4.7.) consists of quartz-hematite aggregate with symplectic structure (light grey – hematite, grey – quartz). With analyzer.

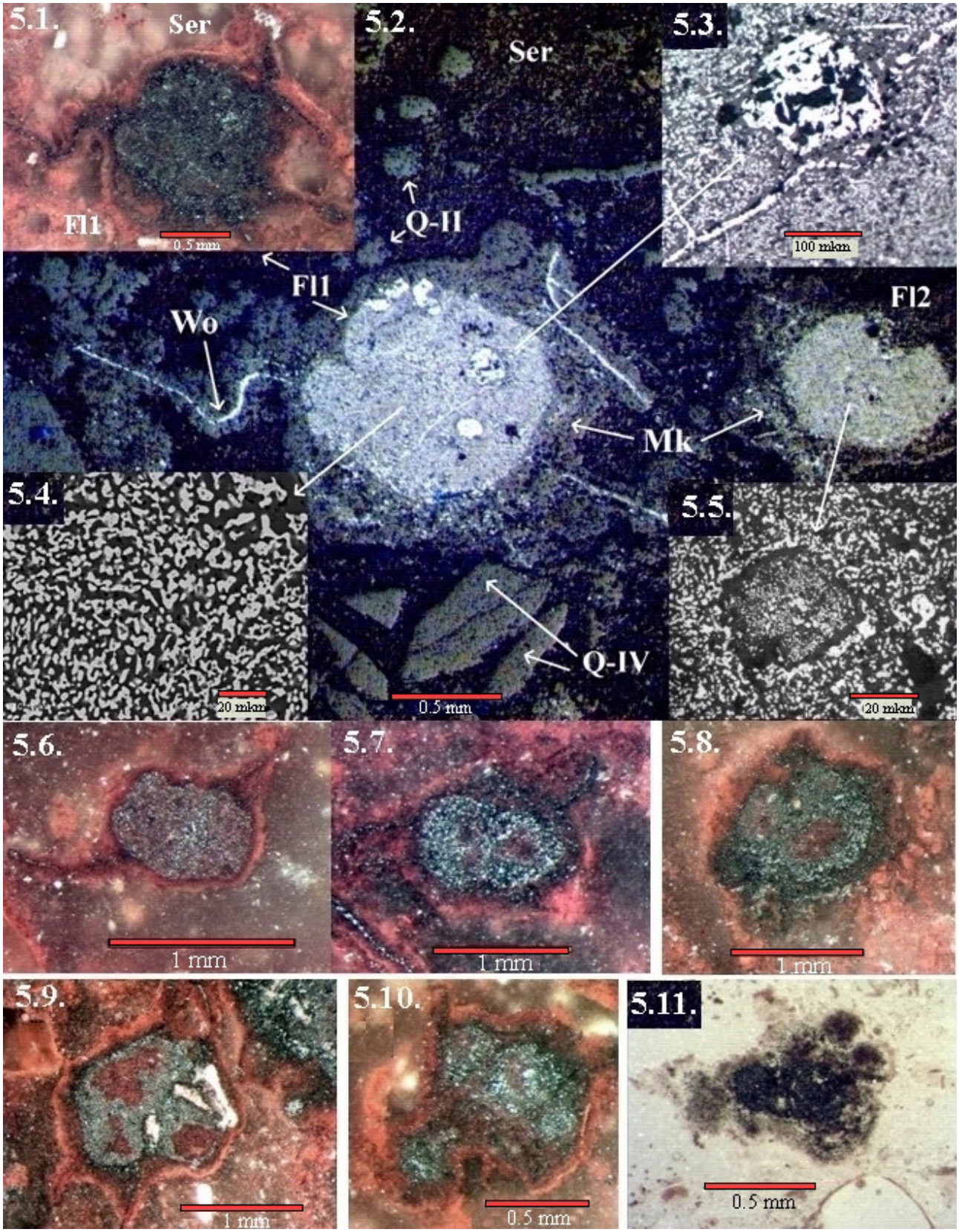

Figure 5: Microphoto of flagellate-like structures (FlS) (5.1-5.6.) and structures are similar to microfossils of multicellular microorganisms (5.7.–5.11.) in the sericite aggregate from cement of breccias in rhyolites under optical microscope.

5.1. Flagellate-like structures (Fl1) with whip-like offshoot consisting of quartz-hematite aggregate in sericite aggregate (Ser). Polished specimen (Ps), without analyzer.

5.2. Two FlS (Fl1 and Fl2) with whip-like offshoot (Wo) consisting of quartz-hematite aggregate (light grey) in sericite aggregate (dark grey). Grey – microquartzites (Mk) surrounding the FlS. Q-II – rounded globules of quartz xenocrysts second generation. Q-IV – clasts of quartz xenocrysts of fourth generation. Ps, with analyzer.

3.1. Two FlS (Fl1 and Fl2) with whip-like offshoot (Wo) consisting of quartz-hematite aggregate (light grey) in dark grey sericite aggregate (Ser). Grey – microquartzites (Mk) surrounding the FlS. Q-II – rounded globules of quartz xenocrysts from second-generation dynamometamorphic rocks. Q-IV – clasts of quartz xenocrysts from fourth-generation rhyolites. Polished specimen (Ps), with analyzer.
3.2. Fl1. Ps, without analyzer.
5.3. Fragments of Fl1 – structure similar to cell nucleus (light grey – hematite, grey – quartz). Ps, with analyzer.
5.4. Fragments of Fl1 – quartz-hematite aggregate with symplectic texture (light grey – hematite 40%, grey – quartz 60%). Microphotographs taken using scanning electron microscope JSM-6510LA.
5.5. Fragments of Fl2 – structure similar to the cells core (light grey – hematite, grey – quartz). Ps, with analyzer.
5.6. FlS with whip-like offshoot consisting of quartz-hematite aggregate (quartz – 80%, hematite – 20%) and surrounded with microquartzites. Ps, without analyzer.
5.7. – 5.10. Structures are similar to microfossils of multicellular microorganisms with whip-like offshoot surrounded by microquartzites. Ps, without analyzer.
5.11. Structure is similar to microfossils of multicellular microorganisms with whip-like offshoot surrounded by microquartzites. Thin section, without the analyzer.